**Abstract** Metamaterials are artificial materials structured on a subwavelength scale to provide electromagnetic properties beyond those available in nature. Progress in this young field has been startlingly swift. The last year alone has seen the realization of the first optical negative-index metamaterials and the constructon of two very striking metamaterial-based devices: an invisibility cloak and a far-field lens capable of subwavelength imaging. Here, I review these developments and the key concepts that made them possible.

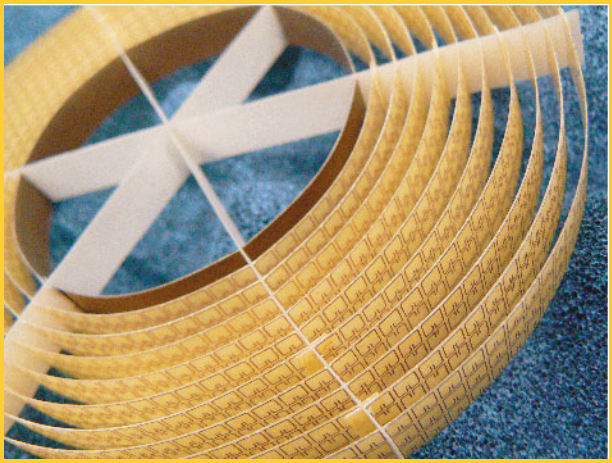

A metamaterial invisibility cloak for microwaves [1].



# Structure and properties of electromagnetic metamaterials

*Ben Wood*

Physics Department, Imperial College London, Exhibition Road, London SW7 2AZ, UK

Received: 23 July 2007, Revised: 11 October 2007, Accepted: 17 October 2007
Published online: 9 November 2007

**Key words:** metamaterials; negative refraction; split ring resonator; homogenization

**PACS:** 41.20.-q, 41.20.Gz, 41.20.Jb, 42.15.Eq, 42.25.-p, 42.30.Va, 42.70.Qs, 42.79.-e, 75.70.Cn, 75.75.+a, 77.22.-d, 77.22.Ch, 78.20.-e, 78.20.Ci, 78.20.Fm, 78.67.Pt, 81.05.Zx

## 1. Introduction

Our ability to manipulate light has traditionally depended on fashioning naturally-occurring materials into useful shapes, like lenses. The set of materials available could only be expanded through chemistry – by making new compounds – but the range of electromagnetic properties remained limited. Metamaterials are a new class of materials which have dramatically increased this range. They take their properties from the structure, as well as the composition, of their constituent elements. A defining property of metamaterials is that the size and spacing of these structural elements should be significantly less than the relevant wavelength of light. They can then be viewed as "artificial atoms", and metamaterials can therefore be described in the same simple and powerful way as natural materials, using only a small number of effective parameters.

The explosion of interest in metamaterials is in large part due to one particular property – a negative refractive index [2] – that cannot be found in natural materials or through chemistry, but has been realized with the help of metamaterials [3, 4]. The discovery that negative refraction allows the creation of a superlens capable of subwavelength imaging [5] has further increased the demand for negative index metamaterials (NIMs).

The topic of metamaterials has grown rapidly in the last ten years, and is now vast. It will not be covered in its entirety here; instead, some important concepts and developments have been selected.

The requirement that the structure must be subwavelength in scale makes it harder to construct metamaterials for high-frequency operation. The first modern metamaterials [6–8] were designed for microwave frequencies. Applications in sensing and telecommunications mean that

e-mail: ben.wood@imperial.ac.uk

this frequency band is technologically important; similarly, magnetic resonance imaging has stimulated research at longer wavelengths [9]. At the same time, the prize of achieving negative refraction with visible light has driven researchers to push metamaterials toward ever-higher frequencies [10], and the first optical NIMs have recently been produced [11].

A promising alternative (but related) route to subwavelength imaging with visible light emerges if the far-field component of the image is neglected. In the near field, the electric and magnetic disturbances decouple, so light of one polarization can be "focused" by a medium with only a negative dielectric permittivity. This is a less challenging requirement than a negative index – even a flat, thin sheet of silver will act as a form of superlens [5, 12]. An improved version of this near-field lens can be made by dividing the metal into layers separated by a conventional dielectric [14]. The layered metamaterial formed in this way can be wrapped around into a cylinder or sphere to make a hyperlens that not only transfers a subwavelength image but also provides magnification [15, 16].

The response of these layered metamaterials to an electric field clearly depends on the direction in which the field is applied: they are highly anisotropic. This ability to tune the response independently in different directions is often desirable. An example is the case of the recently-demonstrated electromagnetic cloak [1, 17], which can hide an object from fields at a certain frequency; the cloaking material has a graded anisotropic response, which cannot be achieved without metamaterials.

The cloak is a product of a new design paradigm called transform optics [17–19]. This generates a recipe for the local electromagnetic properties required to mimic a given warping of space. These recipes invariably call for anisotropic media, and metamaterials are uniquely positioned to meet this demand.

## 2. Homogenization and effective medium parameters

What constitutes a metamaterial? The term was coined in 2000 [20] and has a different meaning for different researchers. However, it is usually taken to mean an artificial material whose properties derive from subwavelength geometric structure, rather than just chemical composition. The restriction that the structure be on a scale smaller than the wavelength is important, and serves to distinguish metamaterials from photonic crystals (in which the structure is on the same scale as the wavelength); metamaterials thus make use of light scattering, while photonic crystals depend on diffraction. The structural elements which make up a metamaterial may be periodic, but are not necessarily so; they are often resonant, but neither is this an absolute requirement.

The power of metamaterials comes from the fact that the response of these (sometimes very complicated) structures can be represented with a very small number of relatively simple parameters. We are accustomed to describing the behaviour of light in natural materials by assigning to them properties like dielectric permittivity $\varepsilon$ and magnetic permeability $\mu$. These properties appear in the constitutive equations which relate the derived fields $\mathbf{D}$ and $\mathbf{H}$ to the macroscopic electric and magnetic fields $\mathbf{E}$ and $\mathbf{B}$; at any given frequency, the equations take the form

$$\begin{aligned} \mathbf{D} &= \varepsilon_0 \boldsymbol{\varepsilon} \mathbf{E} + \sqrt{\varepsilon_0 \mu_0}\, \boldsymbol{\xi} \mathbf{H}\,, \\ \mathbf{B} &= \sqrt{\varepsilon_0 \mu_0}\, \boldsymbol{\zeta} \mathbf{E} + \mu_0 \boldsymbol{\mu} \mathbf{H} \end{aligned} \tag{1}$$

in general bianisotropic linear media. The dimensionless tensors $\boldsymbol{\xi}$ and $\boldsymbol{\zeta}$ describe any magnetoelectric coupling (gyrotropy); like $\boldsymbol{\varepsilon}$ and $\boldsymbol{\mu}$, they may be complex, reflecting possible phase differences between the fields, and vary with frequency.

We are able to parameterize the response of a complicated system in this very simple way because the macroscopic fields represent averages in which atomic-scale fluctuations are washed out. The averaging is performed on a scale set by the wavelength of light in question; in order for it to be valid, the volume of a region of this size must contain a large number of atoms. We can apply the same treatment to metamaterials as long as the spacing of the structural elements – the artificial atoms – remains significantly smaller than the wavelength of light.

Evidently, some procedure is required for determining the effective medium parameters, and various methods have been employed to this end. For some simple cases, such as composites – disordered mixtures of two or more materials – analytical formulas are available. The homogenization of composites has a long history, dating back at least as far as the mid-19th century, and several formulas (with different domains of applicability) have been developed [21, 22]. The formulas involve weighted averages of the properties of the individual materials, depending on the relative amount of each, and are derived by considering the response of spherical grains or inclusions to an applied field. The subsequent polarization (or magnetization) contributes to the local field experienced by the other grains, which must therefore be solved for in a self-consistent way. More refined versions consider ellipsoidal grains [23].

However, the internal structure of most metamaterials is more complicated than this, and analytical calculations must then be supplemented by numerical simulations. Even here, there are several ways to proceed.

One way to investigate the electromagnetic properties of a material experimentally is to study the amount of light reflected and transmitted by a sample (usually a flat, thin sheet). This kind of experiment can be easily simulated using a finite-difference time-domain program. The transmission and reflection coefficients ($S$ parameters) derive from the material properties and the mapping can be inverted to allow these properties to be determined; this is known as $S$-parameter retrieval [24, 25]. However, there

 

are complicating factors. The first is the nature of the mapping, which is not one-to-one: the square root and inverse cosine functions which appear in the formulas have multiple branches. The second is the choice of boundaries. Metamaterials do not always have clearly-defined edges, and the phase of the transmission and reflection coefficients depend on the width of the sample. By considering slabs of varying thickness and ensuring consistency between the derived parameters, these difficulties can be overcome [26]. However, a general bianisotropic metamaterial can have up to 72 parameters (9 components for each of the tensors $\boldsymbol{\varepsilon}$, $\boldsymbol{\mu}$, $\boldsymbol{\zeta}$ and $\boldsymbol{\xi}$) which must be determined, and a lot of data is therefore required. For complex anisotropic systems, unless many properties can be established in advance – perhaps from symmetry arguments [27, 28] – the transmission and reflection coefficients for normally incident light provide insufficient information. Data for light incident at a range of oblique angles is needed. Having accumulated this data, calculating the effective medium parameters remains a formidable task; a systematic approach based on a combination of stochastic and simplex optimization is one solution [29].

An alternative is to consider the fields inside the theoretical infinite metamaterial. These may not always be accessible experimentally, but computer simulations provide accurate estimates in most cases. The question is then what averaging procedure to use to obtain the effective medium parameters. A simple volume average is not good enough. To see why, consider a cell containing a thin conducting rod (or ring): even for vanishing conductor volume, there can be a finite electric (or magnetic) dipole moment. Volume averaging would suggest that such a system behaves like free space, which is certainly not the case.

One straightforward but effective averaging method suitable for periodic metamaterials has been derived from a finite-difference scheme [30]. In a periodic medium, the propagating solutions of Maxwell's equations take the form of a product: a function with the periodicity of the structure is multiplied by a phase factor $e^{i\mathbf{q}\cdot\mathbf{x}}$. The wave vector $\mathbf{q}$ is thus defined in terms of the phase advance of the fields over a unit cell. The relationship between $\mathbf{q}$ and the frequencies for which propagating solutions exist is called the band structure. Each of these solutions has a different field pattern; in this scheme, the fields are averaged as follows:

$$\begin{aligned}
\bar{E}_i &= \frac{1}{d_i}\int \mathbf{E}\cdot d\mathbf{x}_i\,,\\
\bar{H}_i &= \frac{1}{d_i}\int \mathbf{H}\cdot d\mathbf{x}_i\,,\\
\bar{D}_i &= \frac{d_i}{V}\int \mathbf{D}\cdot d\mathbf{s}_i\,,\\
\bar{B}_i &= \frac{d_i}{V}\int \mathbf{B}\cdot d\mathbf{s}_i\,.
\end{aligned} \tag{2}$$

The averaging is performed along a line for $\bar{\mathbf{E}}$ and $\bar{\mathbf{H}}$ but over a surface for $\bar{\mathbf{D}}$ and $\bar{\mathbf{B}}$. $d_i$ is the length of the unit cell in the $i$ direction and $V$ is the cell volume. The averaged fields are then compared with (1) to calculate $\boldsymbol{\varepsilon}$ and $\boldsymbol{\mu}$ (and $\boldsymbol{\xi}$ and $\boldsymbol{\zeta}$ where appropriate).

## 3. Negative index materials

The subject of negative refractive index is intimately linked with metamaterials. This physical phenomenon was theoretically predicted and analysed long ago, notably by Veselago [2], but remained beyond the reach of experiments until the advent of metamaterials and the increased range of electromagnetic properties they provide. It has been the driving force behind a great deal of research into metamaterials.

In a homogeneous, isotropic medium in the absence of magnetoelectric coupling, the refractive index is

$$n = \pm\sqrt{\varepsilon\mu}\,, \tag{3}$$

where $\varepsilon$ and $\mu$ are now scalars. When $\varepsilon$ and $\mu$ are real and positive, the positive square root is taken, giving a positive real value of $n$. However, when both are negative, the negative root should be chosen [31], giving a negative value of $n$ – and opening the door to a range of unusual and exotic effects.

When light passes from a positive ($n > 0$) to a negative ($n < 0$) medium, Snell's law implies that the angle of refraction is negative. The law remains correct: the refracted ray emerges on the same side of the normal as the incident ray (Fig. 1). Negative refraction has been demonstrated experimentally at microwave frequencies [4, 32] with the help of metamaterials.

In order to satisfy the boundary conditions at the interface between positive and negative media, the component of the wave vector parallel to the interface must be conserved. The wave vector in the NIM therefore points towards the interface, and phase fronts appear to travel in this direction (Fig. 1). However, the direction of energy flow must be away from the boundary. This brings us to a key characteristic of NIMs: the phase velocity points in the opposite direction to the group velocity (which gives the energy flow). This "backward" wave propagation is not unique to NIMs [33]. If we compare the sign of the phase velocity

$$v_\mathrm{p} = \frac{\omega}{k} = \frac{c}{n} \tag{4}$$

with that of the group velocity

$$v_\mathrm{g} = \frac{d\omega}{dk} = \frac{c}{n+\omega\frac{dn}{d\omega}}\,, \tag{5}$$

we see that we can still have backward waves when $n$ is positive as long as

$$\frac{dn}{d\omega} < -\frac{n}{\omega}\,. \tag{6}$$

This is historically known as anomalous dispersion, and is very common; it appears at frequencies close to absorption

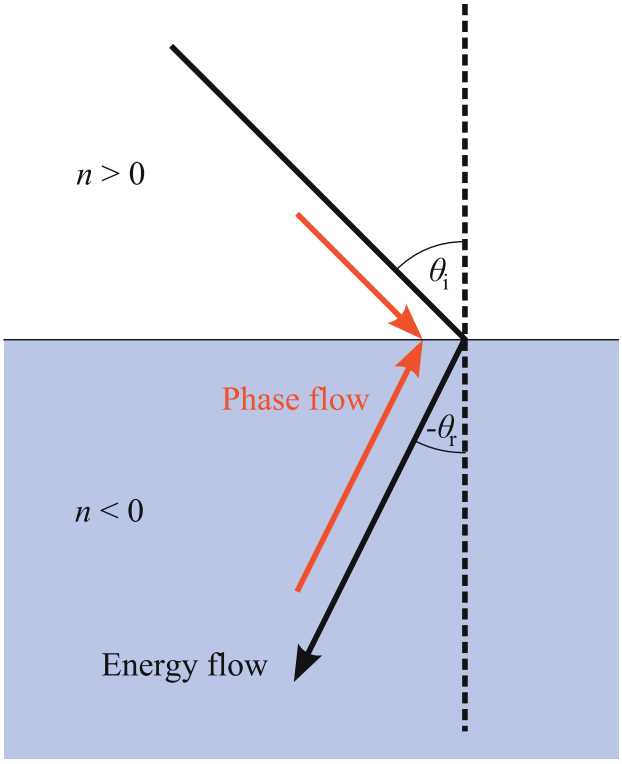


**Figure 1** Negative refraction: light passing from a medium with $n > 0$ to one in which $n < 0$.

bands, where it is naturally accompanied by high absorption.

In NIMs, however, $n < 0$ and $v_p$ has a negative sign; $v_g$ must then be positive. We thus require

$$\frac{dn}{d\omega} > -\frac{n}{\omega}. \tag{7}$$

Note that (7) is *necessary* in order to satisfy the boundary conditions at an interface as long as $n < 0$, while (6) is purely a condition for backward waves in positive media. In NIMs, waves are always backwards. A more careful discussion of this topic also considers the effect of losses and correspondingly complex-valued permittivity and permeability [34]. Note that while significant losses are inevitable in the case of anomalous dispersion, there is no fundamental minimum amount of loss in NIMs.

If the refractive index takes a negative value at some given frequency, (7) shows that it must be dispersive; $n$ decreases as $\omega$ decreases, becoming more negative and eventually diverging. In fact, the effective medium description of the NIM breaks down before this happens, as soon as the wavelength $\lambda/|n|$ becomes comparable with the spacing or size of the elements which make up the material. Nonetheless, this is a clear indication that a negative refractive index depends on resonant behaviour. If $n$ diverges as a function of frequency, the wave vector must also diverge; for a small change in $\omega$, there is a large change in $k$. In other words, many states are contained in a small frequency range – the density of states is high.

We have seen that the group and phase velocities are oppositely-directed in NIMs. The direction of electromagnetic energy flow is determined by the Poynting vector; for propagating plane waves in isotropic media with no magnetoeletric coupling, this is

$$\mathbf{S} = \frac{1}{2\omega\mu_0\mu}\mathbf{k}|\mathbf{E}|^2 = \frac{1}{2\omega\varepsilon_0\varepsilon}\mathbf{k}|\mathbf{H}|^2. \tag{8}$$

When $\varepsilon$ and $\mu$ are both negative, the energy flow is in the opposite direction to $\mathbf{k}$. (If only one is negative, the wave is evanescent, and transports no energy.) In positive media, $\mathbf{E}$, $\mathbf{H}$ and $\mathbf{S}$ form a right-handed triple of vectors; in NIMs, they form a left-handed triple. For this reason, they are sometimes known as left-handed media, although this invites confusion with chiral materials.

Perhaps the most important feature of NIMs is the possibility of making a flat lens with subwavelength imaging properties. Fig. 2 shows a slab made of a material in which $\varepsilon$ and $\mu$ simultaneously take on values close to -1, surrounded by vacuum. Negative refraction at the boundaries means that light rays are brought to a focus twice – once inside the slab and once outside [2]. There are no reflections at the boundaries, because the impedance of the lens material is matched to the vacuum. More importantly, the lens also couples to the near field of the object, which contains all the information about subwavelength detail – information which is lost by conventional lenses. The evanescent components of the field are amplified within this lens and restored in the image plane, thus providing a

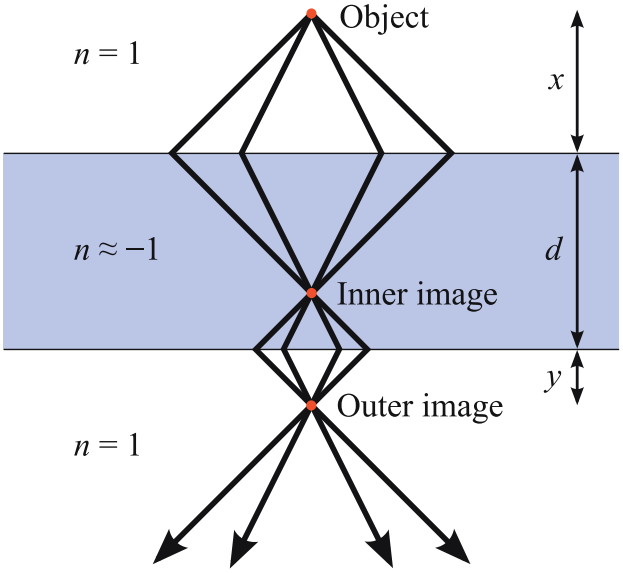


**Figure 2** A NIM lens: light from a point source is refracted at the boundaries to generate two images. The separation of object and image is twice the width of the lens, so that $x + y = d$.

perfect image. The mechanism for this amplification is the stimulation of surface resonances [35, 36].

The realization that the NIM lens could produce an image with subwavelength resolution [5] sparked an enormous amount of research and some heated debate [37]. To say that the image is perfect is, of course, an exaggeration; whereas there is in principle nothing to prevent the refractive index from being both negative and purely real, losses (which degrade the image) are inevitable in practice. In fact losses are necessary to prevent the infinite accumulation of energy on the image-side interface of the lens. They also determine the time required to establish the image; a sharper resonance with lower losses needs more energy input and takes longer to build up. The effect of losses on the image is more destructive for thicker lenses [38] – this kind of flat lens works best when object and image are close together on a scale determined by the wavelength.

Negative refraction has been a central theme in metamaterials research; next, we will examine the resonant structures that have been designed to achieve it.

## 4. Resonant structural elements

In order to demonstrate negative refraction, the permittivity and permeability must be simultaneously negative within some frequency range. But what does a negative permittivity or permeability entail? These quantities describe the effective polarization and magnetization of a medium in response to an applied field. A negative value corresponds to *overscreening*.

As an example, consider a conventional dielectric material composed of an assembly of isotropic polarizable molecules. The molecules behave like a coupled resonators: in equilibrium, they are unpolarized, so there is a restoring force when they are driven by an electric field, and each induced dipole moment also contributes to the total field. The example serves to illustrate both the behaviour of a generic system of resonant elements and the physical implications of different values of $\varepsilon$. The permittivity relates the polarization to the macroscopic field:

$$\mathbf{P} = \varepsilon_0(\varepsilon - 1)\mathbf{E}. \tag{9}$$

In a low-frequency field, the molecules develop dipole moments which are aligned with the electric field vector; the resulting polarization is described by a real permittivity with value greater than one and the field does no net work on the molecules. As the frequency increases, the dipole moments begins to lag behind the field. This phase difference allows work to be done; energy is lost by the field to the molecules and $\varepsilon$ acquires an imaginary part. This imaginary part (and the associated losses) are greatest at the resonant frequency, as is the magnitude of the polarization. At higher frequencies, the dipoles move in antiphase with the applied field; the permittivity is now less than one and almost purely real once more.

The example shows that for the permittivity to be negative, the polarization must be large ($|\mathbf{P}| > \varepsilon_0|\mathbf{E}|$) and in antiphase with the electric field. It also demonstrates the wide range of responses available from a system of coupled resonators, depending on the driving frequency.

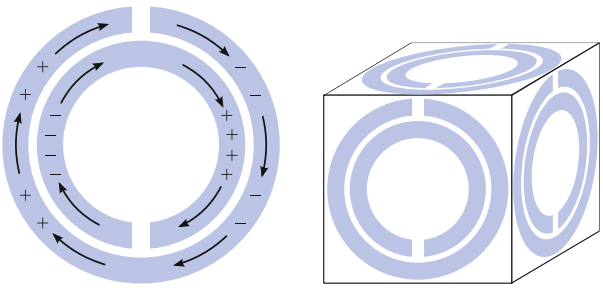

**Figure 3** (Left) The split-ring resonator. The arrows show the currents induced by a magnetic field perpendicular to the conducting rings. Current is permitted to flow around the loop because of the capacitance between the rings; the associated accumulation of charge is also shown. (Right) To make an isotropic metamaterial, the resonators are stacked in a three-dimensional lattice.

Many metamaterials are designed to mimic this basic structure. Elements with a resonant polarization or magnetization response (or both) are combined to produce a wide range of effective values of $\varepsilon$ and $\mu$ (and $\xi$ and $\zeta$ in some cases).

We begin by describing the most ubiquitous of metamaterial elements, the split-ring resonator (SRR). First conceived for use in magnetic resonance work [39], the design was brought to widespread attention when it was introduced in a seminal paper [8] as a means of achieving magnetism at microwave frequencies, above the range of most naturally-occurring magnetic activity. The basic structural unit consisting of a pair of cut rings of conducting material is is shown in Fig. 3. When a changing magnetic field is applied in a direction perpendicular to the rings, it generates currents flowing around them; these currents are interrupted by the gaps, but the large capacitance between the rings acts to complete the circuit. The overall effect is to mimic an LC circuit with a resonant frequency given approximately by [40, 41]

$$\omega_0 = \sqrt{\frac{2}{\pi r L\, C}} \tag{10}$$

where $r$ is the radius of the rings, $L$ the inductance and $C$ the capacitance per unit length. SRRs only respond to magnetic fields applied in the direction normal to the rings; to make an isotropic metamaterial, the SRRs are assembled into a lattice, as shown in Fig. 3. The effective permeability of the resulting medium has the generic form [3, 8]

$$\mu = 1 - \frac{F\omega^2}{\omega^2 - \omega_0^2 + i\omega\Gamma} \tag{11}$$

where $F$ is the fraction of the area of the unit cell occupied by the rings and $\Gamma$ represents (principally radiative) losses.

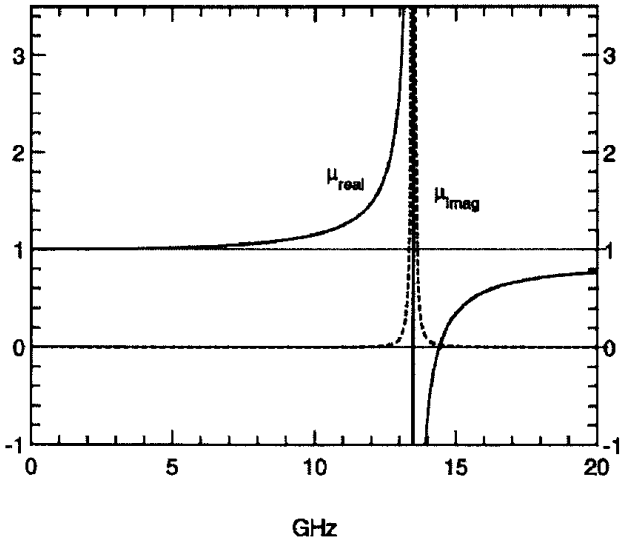


**Figure 4** The effective permeability of the SRR metamaterial as a function of frequency [8]. Losses are dictated by the imaginary part of $\mu$, denoted by the dashed line.

This behaviour, which is characteristic of a resonant system, is plotted in Fig. 4.

A single split ring functions as a resonator, so why use two? When two rings are coupled together, the two principal resonances hybridize and the frequency of the lowest resonance is reduced. For operation at higher frequencies, two rings are no longer the best solution, as we will see.

In fact, the SRR metamaterial is rather more complicated than initial analysis suggested. Several resonances are supported [42], although only the first is amenable to an effective medium description. The rings also display a resonant response to an electric field applied in line with the gaps. The electric and magnetic responses are coupled: the flow of current associated with a magnetic moment is accompanied by the accumulation of charge associated with an electric polarization. The system is therefore bianisotropic [43–45].

One way to regard the electromagnetic coupling is as a consequence of the lack of mirror symmetry of the SRR about the plane normal to the line joining the two gaps [27]. To negate the bianisotropy we can impose this missing symmetry by various means: we can reverse the orientation of the resonators in alternate cells [45] or we can use an inherently symmetrical unit like the broadside-coupled SRR [43].

Fig. 4 shows that within a certain frequency range close to the resonant frequency the effective permeability of the SRR metamaterial takes on a wide range of values. This is the advantage of using resonant elements. The disadvantages are demonstrated in the figure, too: close to the resonance, the permeability disperses very strongly with frequency and has a large imaginary part, indicating that losses are significant here. However, by using nonmagnetic conductors to produce magnetism on a macroscopic scale, the SRRs achieved an important goal – negative permeability, something not found in natural materials.

In contrast, negative permittivity does occur naturally, at least at certain frequencies. Once again, conductors are involved: ordinary metals are described by essentially real and negative values of $\varepsilon$ when interacting with visible light. At lower frequencies, damping becomes more important, so that $\varepsilon$ is typically dominated by losses for microwaves and below. The frequency scale is set by the plasma frequency (the natural frequency of collective bulk charge oscillations), which marks the change from negative (below $\omega_{\mathrm{p}}$) to positive $\varepsilon$:

$$\omega_{\mathrm{p}} = \sqrt{\frac{ne^2}{\varepsilon_0 m}}, \tag{12}$$

A simple way to move the plasma frequency downwards is to replace the bulk metal with thin wires in a grid [7]. This reduces the electron number density, $n$, while at the same time, because of the self-inductance of the wires, the effective electron mass $m$ is increased. The result is a negative-permittivity metamaterial for microwaves. In tandem with SRRs, the wire mesh allowed the first experimental realizaton of a NIM [3, 4].

Here, too, closer inspection revealed that there was more to the wire structure than meets the eye. The 3D wires support an additional and unwanted transmission-line mode [46] which cannot satisfactorily be described by a local effective permittivity. In this mode, the response is nonlocal: the polarization at any point depends not only on the electric field at that point but also the field elsewhere. This phenomenon is known as spatial dispersion, and is inevitable for all materials at high frequencies.

It can be incorporated in a model by introducing an electric permittivity which now depends on the wave vector as well as the frequency [47]. The magnetic permeability then becomes redundant (in the absence of naturally magnetic materials). This approach to homogenization is certainly more general than the local model [48], but loses the advantage of simplicity; boundary conditions are significantly more difficult to implement for spatially-dispersive media.

The wire and SRR metamaterials were designed to work for microwaves. The demand for metamaterials that operate at higher frequencies is great – in particular magnetic metamaterials, because naturally-occurring magnetism is not available in this regime. When moving to higher frequencies, the structural elements must be made smaller to comply with the requirement of subwavelength size. A first step in this direction is therefore to take existing designs and scale them down; accordingly, split-ring resonators have been produced on increasingly small scales [49–52], with resonant frequencies as high as 200 THz. In the process, the double rings have become single, and square-shaped; this simplifies the fabrication considerably, which is an important consideration for these nanoscale systems. The remaining capacitance is

now purely across the gap. Variations on the single ring have been proposed, such as rings with multiple cuts and a higher degree of symmetry to avoid magnetoelectric coupling [53].

Several theoretical studies have investigated just how far this design can be pushed [53, 54]. When the rings are large, both the capacitance and inductance of the circuit scale linearly with the ring size [55]. This happy situation means that as the size is reduced, the resonant frequency increases at exactly the right rate to preserve the ratio of wavelength to structure size, so that the effective medium approximation remains valid. However, this cannot last forever, and a number of factors conspire to put a halt to the scaling. To support a current $I$ flowing around the ring, an amount of magnetic energy $\frac{1}{2}LI^2$ is required, where $L$ is the inductance. $L$ includes a geometric component, which scales linearly with the ring size, and a component due to the self-inductance of the electrons, which scales in *inverse* proportion to the ring size, and therefore becomes progressively more important as this size is reduced. The result is that the resonant frequency saturates, tending to a constant value for small rings. In addition, the increased scattering of electrons at the surface becomes more important, leading to greater losses, and the relative skin depth increases – with the same result [53].

More recent designs have left the ring behind altogether. Pairs of strips [56–58], rods [59–62], and ellipsoidal [63, 64] or rectangular voids [11, 65–67] ("fishnets") have all been employed as the fundamental resonant units of metamaterials (Fig. 5). The designs have much in common. All are based on pairs of elements and seek to achieve a negative permeability by exploiting a resonant mode with asymmetric current flow within each pair. They each exhibit a strong electric as well as magnetic response; all are two-dimensional, and the arrays of voids in metal can be related to those of metal components in dielectric by Babinet's principle.

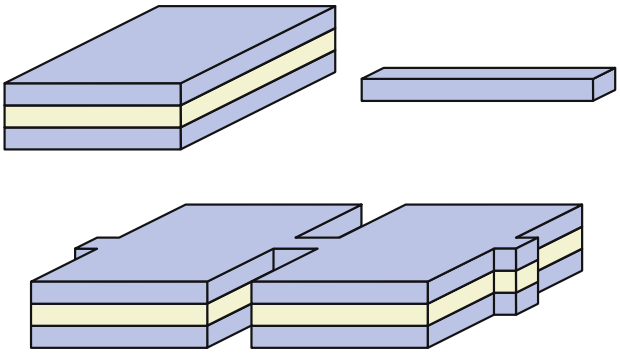

**Figure 5** An example of a design for a high-frequency NIM [67]. Above left is a resonant element consisting of a pair of metal stripes separated by a dielectric layer, which is designed to give $\mu < 0$; above right is a thin metallic wire with $\varepsilon < 0$. Below, the two components are combined in a lattice to form a metamaterial with $n < 0$ in the near-infrared.

The ultimate goal of this area of research is to create an optical NIM. To this end, the paired elements (which give $\mu < 0$ over a limited frequency range) are combined with some kind of metallic background, perhaps in the form of wires, which provides a small, negative permittivity. NIMs have just begun to enter the realm of visible light: to date, the shortest wavelength for which a negative index has been demonstrated is 780 nm [11], using the fishnet structure. A key challenge here is to minimize losses; the figure of merit, $F = |n'|/n''$ should be as large as possible. For the 780 nm NIM, $F$ stands at 0.5, although a value of 3 has been obtained for a wavelength of 1400 nm [65]. The various approaches to optical NIMs have been compared in a recent review [10].

The two-dimensional nature of these metamaterials makes them inherently anisotropic. This is a consequence of the difficulty of manufacturing three-dimensional elements on the nanometre scale rather than a desirable feature. However, for many applications, anisotropy is necessary, and we will now review some metamaterials which incorporate it into their design.

## 5. Anisotropic metamaterials

The usefulness of metamaterials extends far beyond negative refraction. However, the first anisotropic metamaterial that we will describe has its orgins in this area – in particular, it is an indirect descendant of the negative-index lens pictured in Fig. 2. This lens functions best when object and image are less than a wavelength apart. In the near zone, close to the source, the electric and magnetic fields are effectively decoupled. If light from the object is resolved into its two polarization components, the $S$-polarized part is almost exclusively magnetic and the $P$-polarized part electric. Thus, in this regime, only $\varepsilon$ is relevant for $P$-polarized light; if we only care about bringing one polarization component to a focus, then negative $n$ is not necessary, only negative $\varepsilon$. This is a considerable relaxation of the rules, and means that a simple thin metal film can function as a "superlens" [5, 12].

A sheet of silver is not a metamaterial. However, it was predicted that the performance of the superlens could be improved [14] by slicing it into layers, alternating metal ($\varepsilon < 0$) with dielectric ($\varepsilon > 0$). Since the layers must be very thin – the thickness of the whole lens should be less than one wavelength – the layered system can be homogenized and treated as an effective medium [68], with an anisotropic effective permittivity

$$\varepsilon_{\parallel} = \frac{1}{2}\left(\varepsilon_{\mathrm{m}} + \varepsilon_{\mathrm{d}}\right) \tag{13}$$

$$\frac{1}{\varepsilon_{\perp}} = \frac{1}{2}\left(\frac{1}{\varepsilon_{\mathrm{m}}} + \frac{1}{\varepsilon_{\mathrm{d}}}\right), \tag{14}$$

assuming the layers are of equal thickness. To operate in the superlens regime, the metal and dielectric permittivities should be equal and opposite (neglecting losses). The

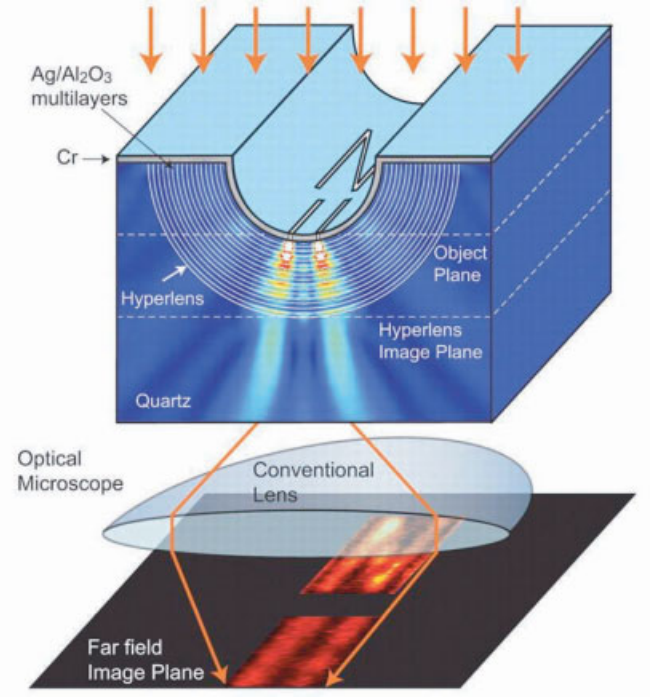


**Figure 6** The hyperlens. Light is coupled from the object, which lies within the half-cylinder, to the exterior of the hyperlens and then focused using a conventional lens. The figure is taken from [15].

in-plane component of the effective permittivity then tends to zero while the perpendicular component diverges. The consequences for wave propagation are revealed by the dispersion relation for $P$-polarized waves:

$$\frac{k_{\parallel}^2}{\varepsilon_{\perp}} + \frac{k_{\perp}^2}{\varepsilon_{\parallel}} = \frac{\omega^2}{c^2}\,, \tag{15}$$

which shows that when $\varepsilon_{\perp} \to \infty$, the phase advance normal to the layers (governed by $k_{\perp}$) is independent of $k_{\parallel}$, and when $\varepsilon_{\parallel} \to 0$ there is no phase advance at all. This is how the layered lens manages to transfer the electric field from object to image.

To go a step further and obtain a magnified image, some curvature is required [69]. By wrapping the layered metamaterial around into a cylindrical or half-cylindrical shell, the image of an object inside the shell is transferred to the outside [70, 71], and is magnified in the process. The magnification turns subwavelength features into superwavelength ones which can then be observed with a conventional lens (Fig. 6). This metamaterial "hyperlens" – so-called because of the hyperbolic shape of the dispersion relation in the layered medium – couples the near field of the object to the far field outside the lens, and has now been realized [15, 16].

The original description of the cylindrical lens used a transformation of the flat lens to derive the appropriate form for $\varepsilon$ and $\mu$ [69]. This technique is an example of a design paradigm called transform optics [17–19, 72, 73]. The idea is simple: starting with some configuration of fields, we imagine warping space to obtain a new, desired configuration; by keeping track of the coordinate transformations performed, we can derive a prescription for the permittivity and permeability (as functions of position) that will mimic this deformation of space. A striking example is the electromagnetic cloak (Fig. 7). Here, the desired effect is to mimic a hole in space: light is guided around the outside, and anything inside is hidden from view.

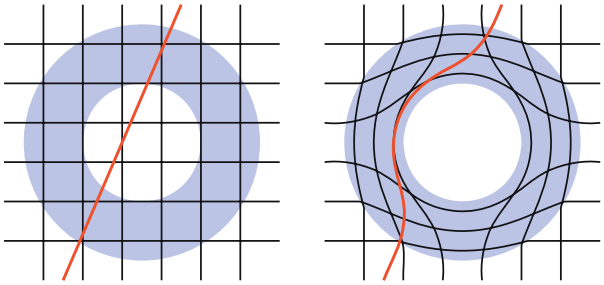

**Figure 7** The cloaking transformation, showing the deformation of a uniform grid. Space is squashed in the radial direction and stretched azimuthally. The red line shows a ray that would have passed through the middle of the cloak being guided around it.

The recipe for the cloak, like all the interesting recipes that derive from this design paradigm, demands materials with highly anisotropic permittivity and permeability. Mimicking the compression of space in direction $i$ requires $0 < \varepsilon_i < 1$ and $0 < \mu_i < 1$, while stretching space dictates that $\varepsilon_i > 1$, $\mu_i > 1$; the symmetry of Maxwell's equations means that $\boldsymbol{\varepsilon}$ and $\boldsymbol{\mu}$ take identical values everywhere.

Even with the help of metamaterials, meeting the exacting requirements of the full theoretical cloak remains an impossible task. However, there are opportunities for simplification: switching to a cylindrical cloak, dealing with just one polarization, and relaxing the constraints to preserve the dispersion relation at the expense of some scattering made the construction of a prototype cloak for microwaves possible [1]. Single SRRs provided the carefully graded, anisotropic electromagnetic response; careful adjustment of the geometric parameters in simulations allowed the effective permittivity and permeability to be controlled, and the cloak was a success.

An alternative way to simplify the problem is to move to zero frequency (DC). In this limit, electric and magnetic fields are decoupled as the wavelength (and the extent of the near zone) diverges. To make a cloak for magnetic fields, we can now forget about $\boldsymbol{\varepsilon}$. However, a metamaterial with a highly anisotropic magnetic response is required: strongly diamagnetic in one direction, and paramagnetic in the others. We can obtain diamagnetism at zero frequency with the help of superconductors, which superficially resemble bulk diamagnets; by chopping the superconductors into cubes, we allow some field penetra-

tion, thus controlling the strength of the effective diamagnetism. By squashing the cubes into plates, the response becomes anisotropic [74]; adding thin layers of strongly paramagnetic material makes the metamaterial complete. This metamaterial is also unusual for another reason – it is not based on resonant elements, and therefore does not suffer the consequent problems of narrow bandwidth and high losses. When $\varepsilon$ and $\mu$ do not have to be negative, resonance is no longer forced upon us, and nonresonant metamaterials have advantages.

The very low frequency regime remains relatively unexplored, although some work has been carried out on radio-frequency metamaterials [9]. Here, the preferred resonant element is the Swiss Roll, which consists of layers of insulated conductor wound in a spiral, and has resonant frequencies of up to 100 MHz. An array of these rolls with all their axes aligned is a highly anisotropic magnetic metamaterial; for this medium, the component of the effective permeability in the direction of the roll axes takes on a wide range of values, both positive and negative. Working at a frequency where this quantity is large and positive, the array of rolls functions as an endoscope for magnetic fields, transferring an image along the length of the rolls [75]. This is not a lens; there is no focusing effect. However, it is possible to construct a near-field lens – the radio-frequency magnetic analogue of the silver superlens – by arranging the rolls in a logpile structure, so that the effective permeability becomes isotropic [76].

## 6. Conclusion

Metamaterials is still a young field – the name itself is less than ten years old – but has already generated a huge body of research, and interest in the area continues to increase. Amazing progress has been made, turning theoretical pipe dreams like negative refraction and invsibility cloaks into experimental reality. There is no doubt that negative refraction has made a significant contribution to the explosion of interest in metamaterials, and it continues to drive a great deal of research, particularly for those working with visible light. However, there is much more ground to investigate: low-frequency, chiral, highly anisotropic and nonresonant metamaterials all hold great promise for the future.

Ben Wood was born in 1978. He received his PhD in physics from Imperial College London in 2005 for investigations into ways of improving electronic structure simulations of quasi-2D systems. After completing his PhD he remained with the Condensed Matter Theory Group at Imperial, where he now works as a postdoctoral researcher studying metamaterials in the team of Prof. Sir John Pendry.

## References


[1] D. Schurig, J. J. Mock, B. J. Justice, S. A. Cummer, J. B. Pendry, A. F. Starr, and D. R. Smith, Metamaterial electromagnetic cloak at microwave frequencies, Science (USA) **314**(5801), 977–980 (2006).

[2] V. G. Veselago, The electrodynamics of substances with simultaneously negative values of $\varepsilon$ and $\mu$, Sov. Phys.-Usp. (USA) **10**, 509–514 (1968).

[3] D. R. Smith, W. J. Padilla, D. C. Vier, S. C. Nemat-Nasser, and S. Schultz, Composite medium with simultaneously negative permeability and permittivity, Phys. Rev. Lett. (USA) **84**(18), 4184–4187 (2000).

[4] C. G. Parazzoli, R. B. Greegor, K. Li, B. E. C. Koltenbah, and M. Tanielian, Experimental verification and simulation of negative index of refraction using snell's law, Phys. Rev. Lett. (USA) **90**(10), 107401 (2003).

[5] J. B. Pendry, Negative refraction makes a perfect lens, Phys. Rev. Lett. (USA) **85**(18), 3966–3969 (2000).

[6] M. M. I. Saadoun and N. Engheta, A reciprocal phase-shifter using novel pseudochiral or omega-medium, Microw. Opt. Technol. Lett. **5**(4), 184–188 (1992).

[7] J. B. Pendry, A. J. Holden, W. J. Stewart, and I. Young, Extremely low frequency plasmons in metallic mesostructures, Phys. Rev. Lett. (USA) **76**(25), 4773–4776 (1996).

[8] J. B. Pendry, A. J. Holden, D. J. Robbins, and W. J. Stewart, Magnetism from conductors and enhanced nonlinear phenomena, IEEE Trans. Microw. Theory Tech. (USA) **47**(11), 2075–2084 (1999).

[9] M. C. K. Wiltshire, Radio frequency (rf) metamaterials, physica status solidi b (Germany) **244**(4), 1227–1236 (2007).

[10] V. M. Shalaev, Optical negative-index metamaterials, Nature Photonics **1**(1), 41–48 (2007).

[11] G. Dolling, M. Wegener, C. M. Soukoulis, and S. Linden, Negative-index metamaterial at 780 nm wavelength, Opt. Lett. (USA) **32**(1), 53–55 (2007).

[12] N. Fang, H. Lee, C. Sun, and X. Zhang, Sub-diffraction-limited optical imaging with a silver superlens, Science (USA) **308**(5721), 534–537 (2005).

[13] E. Shamonina, V. A. Kalinin, K. H. Ringhofer, and L. Solymar, Imaging, compression and poynting vector streamlines for negative permittivity materials, Electronics Letters, **37**(20), 1243 (2001).

[14] S. A. Ramakrishna, J. B. Pendry, M. C. K. Wiltshire, and W. J. Stewart, Imaging the near field, J. Mod. Opt. (UK) **50**(9), 1419–1430 (2003).

[15] Z. W. Liu, H. Lee, Y. Xiong, C. Sun, and X. Zhang, Far-field optical hyperlens magnifying sub-diffraction-limited objects, Science (USA) **315**(5819), 1686–1686 (2007).

[16] I. I. Smolyaninov, Y. J. Hung, and C. C. Davis, Magnifying superlens in the visible frequency range, Science (USA) **315**(5819), 1699–1701 (2007).

[17] J. B. Pendry, D. Schurig, and D. R. Smith, Controlling electromagnetic fields, Science (USA) **312**(5781), 1780–1782 (2006).

[18] A. J. Ward and J. B. Pendry, Refraction and geometry in maxwell's equations, J. Mod. Opt. (UK) **43**(4), 773–793 (1996).

[19] D. Schurig, J. B. Pendry, and D. R. Smith, Calculation of material properties and ray tracing in transformation media, Opt. Express (USA) **14**(21), 9794–9804 (2006).

[20] R. M. Walser, Electromagnetic metamaterials, in: Proceedings of SPIE, Vol. 4467 of Complex Mediums II: Beyond Linear Isotropic Dielectrics, edited by Akhlesh Lakhtakia, Werner S. Weiglhofer, and Ian J. Hodgkinson (2001), pp. 1–15 .
[21] J. C. Maxwell Garnett, Colours in metal glasses and metal films, Trans. R. Soc., **CCIII**, 385–420 (1904).
[22] D. A. G. Bruggeman, Berechnung verschiedener physikalischer Konstanten von heterogenen Substanzen. I. Dielektrizitätskonstanten und Leitfähigkeiten der Mischkörper aus isotropen Substanzen, Ann. Phys. (Leipzig) **416**(7), 636–664 (1935).
[23] A. Sihvola, Mixing rules with complex dielectric coefficients, Subsurf. Sens. Technol. Appl. **1**, 393–415 (2000), [1].
[24] W. B. Weir, Automatic measurement of complex dielectric constant and permeability at microwave frequencies, Proc. IEEE **62**(1), 33–36 (1974).
[25] D. R. Smith, S. Schultz, P. Markos, and C. M. Soukoulis, Determination of effective permittivity and permeability of metamaterials from reflection and transmission coefficients, Phys. Rev. B (USA) **65**(19), 195104 (2002).
[26] X. D. Chen, T. M. Grzegorczyk, B. I. Wu, J. Pacheco, and J. A. Kong, Robust method to retrieve the constitutive effective parameters of metamaterials, Phys. Rev. E (USA) **70**(1), 016608 (2004), Part 2.
[27] W. J. Padilla, Group theoretical description of artificial electromagnetic metamaterials, Opt. Express (USA) **15**(4), 1639–1646 (2007).
[28] D. R. Smith, D. Schurig, and J. J. Mock, Characterization of a planar artificial magnetic metamaterial surface, Phys. Rev. E (USA), **74**(3), 036604 (2006), Part 2.
[29] X. Chen, T. M. Grzegorczyk, and J. A. Kong, Optimization approach to the retrieval of the constitutive parameters of a slab of general bianisotropic medium, Progr. Electromagn. Res.-Pier **60**, 1–18 (2006).
[30] D. R. Smith and J. B. Pendry, Homogenization of metamaterials by field averaging (invited paper), J. Opt. Soc. Am. B, Opt. Phys. (USA) **23**(3), 391–403 (2006).
[31] R. W. Ziolkowski and E. Heyman, Wave propagation in media having negative permittivity and permeability, Phys. Rev. E (USA) **64**(5), 056625 (2001), Part 2.
[32] R. A. Shelby, D. R. Smith, and S. Schultz, Experimental verification of a negative index of refraction, Science (USA) **292**(5514), 77–79 (2001).
[33] A. D. Boardman, N. King, and L. Velasco, Negative refraction in perspective, Electromagnetics (USA) **25**(5), 365–389 (2005).
[34] M. W. McCall, A. Lakhtakia, and W. S. Weiglhofer, The negative index of refraction demystified, Eur. J. Phys. (UK) **23**(3), 353–359 (2002).
[35] R. Ruppin, Surface polaritons of a left-handed medium, Phys. Lett. A, **277**, 61–64 (2000).
[36] R. Ruppin, Surface polaritons of a left-handed material slab, J. Phys., Condens. Matter. (UK) **13**, 1811–1819 (2001).
[37] N. Garcia and M. Nieto-Vesperinas, Left-handed materials do not make a perfect lens, Phys. Rev. Lett. (USA) **88**(20), 207403 (2002).
[38] V. A. Podolskiy and E. E. Narimanov, Near-sighted superlens, Opt. Lett. (USA) **30**(1), 75–77 (2005).
[39] W. N. Hardy and L. A. Whitehead, Split-ring resonator for use in magnetic-resonance from 200–2000 MHz, Rev. Sci. Instrum. **52**(2), 213–216 (1981).
[40] R. Marques, F. Mesa, J. Martel, and F. Medina, Comparative analysis of edge- and broadside-coupled split ring resonators for metamaterial design – theory and experiments, IEEE Trans. Antennas Propag. (USA) **51**(10), 2572–2581 (2003), Part 1.
[41] M. Shamonin, E. Shamonina, V. Kalinin, and L. Solymar, Resonant frequencies of a split-ring resonator: Analytical solutions and numerical simulations, Microw. Opt. Technol. Lett. **44**(2), 133–136 (2005).
[42] J. Garcia-Garcia, F. Martin, J. D. Baena, R. Marques, and L. Jelinek, On the resonances and polarizabilities of split ring resonators, J. Appl. Phys. (USA) **98**(3), 033103 (2005).
[43] R. Marques, F. Medina, and R. Rafii-El-Idrissi, Role of bianisotropy in negative permeability and left-handed metamaterials, Phys. Rev. B (USA) **65**(14), 144440 (2002).
[44] B. Sauviac, C. R. Simovski, and S. A. Tretyakov, Double split-ring resonators: Analytical modeling and numerical simulations, Electromagnetics (USA) **24**(5), 317–338 (2004).
[45] D. R. Smith, J. Gollub, J. J. Mock, W. J. Padilla, and D. Schurig, Calculation and measurement of bianisotropy in a split ring resonator metamaterial, J. Appl. Phys. (USA) **100**(2), 024507 (2006).
[46] P. A. Belov, R. Marques, S. I. Maslovski, I. S. Nefedov, M. Silveirinha, C. R. Simovski, and S. A. Tretyakov, Strong spatial dispersion in wire media in the very large wavelength limit, Phys. Rev. B (USA) **67**(11), 113103 (2003).
[47] L. D. Landau, E. M. Lifshitz, and L. P. Pitaevskii, Electrodynamics of Continuous Media, Course of Theoretical Physics, Vol. 8, 2nd ed. (Pergamon Press, Oxford, 1984).
[48] M. G. Silveirinha, Metamaterial homogenization approach with application to the characterization of microstructured composites with negative parameters, Phys. Rev. B (USA) **75**(11), 115104 (2007).
[49] T. J. Yen, W. J. Padilla, N. Fang, D. C. Vier, D. R. Smith, J. B. Pendry, D. N. Basov, and X. Zhang, Terahertz magnetic response from artificial materials, Science (USA) **303**(5663), 1494–1496 (2004).
[50] N. Katsarakis, G. Konstantinidis, A. Kostopoulos, R. S. Penciu, T. F. Gundogdu, M. Kafesaki, E. N. Economou, T. Koschny, and C. M. Soukoulis, Magnetic response of split-ring resonators in the far-infrared frequency regime, Opt. Lett. (USA) **30**(11), 1348–1350 (2005).
[51] S. Linden, C. Enkrich, M. Wegener, J. F. Zhou, T. Koschny, and C. M. Soukoulis, Magnetic response of metamaterials at 100 terahertz, Science (USA) **306**(5700), 1351–1353 (2004).
[52] C. Enkrich, M. Wegener, S. Linden, S. Burger, L. Zschiedrich, F. Schmidt, J. F. Zhou, T. Koschny, and C. M. Soukoulis, Magnetic metamaterials at telecommunication and visible frequencies, Phys. Rev. Lett. (USA) **95**(20), 203901 (2005).
[53] J. Zhou, T. Koschny, M. Kafesaki, E. N. Economou, J. B. Pendry, and C. M. Soukoulis, Saturation of the mag-

 

netic response of split-ring resonators at optical frequencies, Phys. Rev. Lett. (USA) **95**(22), 223902 (2005).
[54] S. O'Brien and J. B. Pendry, Magnetic activity at infrared frequencies in structured metallic photonic crystals, J. Phys., Condens. Matter. (UK) **14**(25), 6383–6394 (2002).
[55] S. Linden, C. Enkrich, G. Dolling, M. W. Klein, J. Zhou, T. Koschny, C. M. Soukoulis, S. Burger, F. Schmidt, and M. Wegener, Photonic metamaterials: Magnetism at optical frequencies, IEEE J. Sel. Top. Quantum Electron. (USA) **12**(6), 1097–1105 (2006), Part 1.
[56] A. V. Kildishev, W. S. Cai, U. K. Chettiar, H. K. Yuan, A. K. Sarychev, V. P. Drachev, and V. M. Shalaev, Negative refractive index in optics of metal-dielectric composites, J. Opt. Soc. Am. B, Opt. Phys. (USA) **23**(3), 423–433 (2006).
[57] G. Shvets and Y. A. Urzhumov, Negative index metamaterials based on two-dimensional metallic structures, J. Opt. A, Pure Appl. Opt. (UK) **8**(4), S122–S130 (2006), Sp. Iss. SI.
[58] H. K. Yuan, U. K. Chettiar, W. Cai, A. V. Kildishev, A. Boltasseva, V. P. Drachev, and V. M. Shalaev, A negative permeability at red light, Opt. Express (USA) **15**(3), 1076–1083 (2007).
[59] A. N. Lagarkov and A. K. Sarychev, Electromagnetic properties of composites containing elongated conducting inclusions, Phys. Rev. B (USA) **53**(10), 6318–6336 (1996).
[60] V. A. Podolskiy, A. K. Sarychev, and V. M. Shalaev, Plasmon modes in metal nanowires and left-handed materials, J. Nonlinear Opt. Phys. Mater. (Singapore) **11**(1), 65–74 (2002).
[61] L. V. Panina, A. N. Grigorenko, and D. P. Makhnovskiy, Optomagnetic composite medium with conducting nanoelements, Phys. Rev. B (USA) **66**(15), 155411 (2002).
[62] V. M. Shalaev, W. S. Cai, U. K. Chettiar, H. K. Yuan, A. K. Sarychev, V. P. Drachev, and A. V. Kildishev, Negative index of refraction in optical metamaterials, Opt. Lett. (USA) **30**(24), 3356–3358 (2005).
[63] S. Zhang, W. J. Fan, N. C. Panoiu, K. J. Malloy, R. M. Osgood, and S. R. J. Brueck, Experimental demonstration of near-infrared negative-index metamaterials, Phys. Rev. Lett. (USA) **95**(13), 137404 (2005).
[64] S. Zhang, W. J. Fan, K. J. Malloy, S. R. J. Brueck, N. C. Panoiu, and R. O. Osgood, Demonstration of metal-dielectric negative-index metamaterials with improved performance at optical frequencies, J. Opt. Soc. Am. B, Opt. Phys. (USA) **23**(3), 434–438 (2006).
[65] G. Dolling, C. Enkrich, M. Wegener, C. M. Soukoulis, and S. Linden, Low-loss negative-index metamaterial at telecommunication wavelengths, Opt. Lett. (USA) **31**(12), 1800–1802 (2006).
[66] G. Dolling, C. Enkrich, M. Wegener, C. M. Soukoulis, and S. Linden, Simultaneous negative phase and group velocity of light in a metamaterial, Science (USA) **312**(5775), 892–894 (2006).
[67] S. Zhang, W. J. Fan, K. J. Malloy, S. R. J. Brueck, N. C. Panoiu, and R. M. Osgood, Near-infrared double negative metamaterials, Opt. Express (USA) **13**(13), 4922–4930 (2005).
[68] B. Wood, J. B. Pendry, and D. P. Tsai, Directed subwavelength imaging using a layered metal-dielectric system, Phys. Rev. B (USA) **74**(11), 115116 (2006).
[69] J. B. Pendry, Perfect cylindrical lenses, Opt. Express (USA) **11**(7), 755–760 (2003).
[70] Z. Jacob, L. V. Alekseyev, and E. Narimanov, Optical hyperlens: Far-field imaging beyond the diffraction limit, Opt. Express (USA) **14**(18), 8247–8256 (2006).
[71] A. Salandrino and N. Engheta, Far-field subdiffraction optical microscopy using metamaterial crystals: Theory and simulations, Phys. Rev. B (USA) **74**(7), 075103 (2006).
[72] U. Leonhardt, Optical conformal mapping, Science (USA) **312**(5781), 1777–1780 (2006).
[73] U. Leonhardt and T. G. Philbin, General relativity in electrical engineering, New J. Phys. **8**, 247 (2006).
[74] B. Wood and J. B. Pendry, Metamaterials at zero frequency, J. Phys., Condens. Matter. (UK) **19**(7), 076208 (2007).
[75] M. C. K. Wiltshire, J. V. Hajnal, J. B. Pendry, D. J. Edwards, and C. J. Stevens, Metamaterial endoscope for magnetic field transfer: near field imaging with magnetic wires, Opt. Express (USA) **11**(7), 709–715 (2003).
[76] M. C. K. Wiltshire, J. B. Pendry, and J. V. Hajnal, Sub-wavelength imaging at radio frequency, J. Phys., Condens. Matter. (UK) **18**(22), L315–L321 (2006).